Bitumen Stabilised Materials: Real Performance Models for BSM-foam Bases

SJ Bredenhann
South African National Roads Agency: Research, Materials and Pavement Design

KJ Jenjins
Stellenbosch University: SANRAL Chair in Pavement Engineering

***Abstract*—The growth in-situ and in-plant recycling units provides evidence of the global increase in application of bitumen stabilisation technology in the rehabilitation of road pavements. Application of the technology has varied regionally and continentally, in terms of mix composition, binder types and application and climatic conditions. So too has the research varied, yielding different mix design methods and structural evaluations procedures.**

In South Africa the vast majority of national roads are constructed with highly compacted granular bases, G1 and G2 in terms of specification, with a stabilised subbase as support. As these pavements near the end of their structural lives a viable rehabilitation strategy is to inject new life into the base by bitumen foam stabilisation. At the same time, the sophistication of laboratory equipment has facilitated more detailed evaluation of material behaviour and performance. This paper uses triaxial testing with advanced instrumentation, to establish the strength (shear parameters), response properties (resilient modulus) and damage properties (permanent deformation) of bitumen stabilised material (BSM). BSM mix compositions typical of southern Africa are used i.e. comprising 2.4% bitumen and 1% cement are evaluated.

The procedure followed in this study was to do triaxial testing on a well-graded, highly compacted granular (G2) material. The same specimens were then stabilised with a bitumen foam process and subjected to the same test regime as the granular material. This allowed the comparison of the granular and foam treated materials' performance.

The primary objective of the study is to compare the performance of a granular material and the foam stabilised version of the same material to mimic an actual real life situation where a road base is initially constructed with a granular material and then, after reaching its structural life, is bitumen-foam stabilised to extend the pavement life.

Results of the study show that the pavement life can be extended with at least the same as the original life. This enables the true benefit, or otherwise, of the bitumen stabilisation to be evaluated.

Keywords— plasticity; granular material; bitumen stabilised materials; stress history; loading cycle; rest periods; relaxation; permanent deformation; design transfer functions

I. INTRODUCTION

The global growth in cold recycling technology as a pavement rehabilitation solution has necessitated the development and refinement of reliable materials performance models and design functions. The increased use of bitumen treated materials (BSM) is evident from the percentage of recyclers with the capacity to stabilise with foamed bitumen and emulsion. In total, approximately 57% of rubber tyre recyclers are able to apply foam or emulsion stabilisation technology.

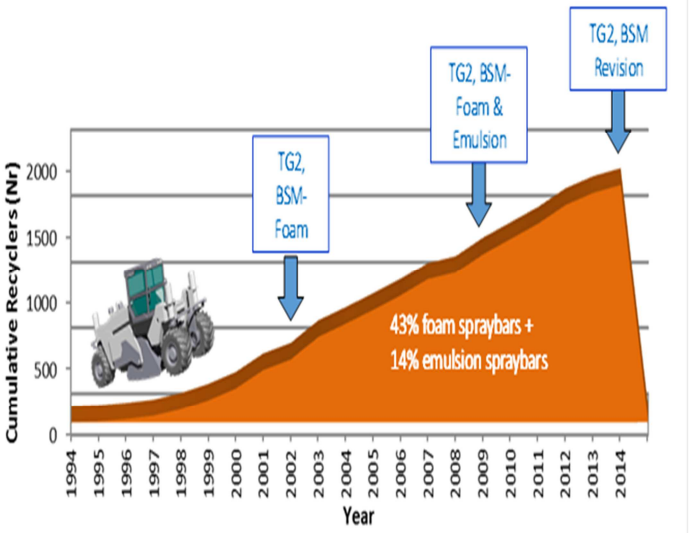

Fig. 1: Global growth in recycler (one brand, rubber tyre only)

During the period of growth of recycling technology, research and construction experience led to the publication of technical documentation. The South African TG2 "Interim guideline Manual for the Design and Use of Foamed Bitumen Treated Materials" (Asphalt Academy, 2002) first addressed BSM-foam technology following the emulsion manuals published earlier (Sabita, 1993 and 1999). This history is outlined in a publication by Jenkins, Collings and Jooste (2008). Subsequently, the TG2 (2009) rewrite included triaxial testing in the mix design phase, with a link to pavement design. At the same time, from 1995 to the present a Cold Recycling Manual has been published by Wirtgen, with periodic updates (2012) which provide useful concepts explaining the behaviour

of the stabilised and cold recycled materials (with active fillers, foamed bitumen or emulsion binders), their mix design and structural performance. These manuals, amongst others, have served the global market for the needs of stabilisation and recycling technology.

There are many parameters that influence the performance of BSMs and these include aggregate origin and properties, volumetric composition, climate, binder and content, binder dispersion, active filler type and content, relative density, moisture content, etc. The complexities of the multi-factorial performance function needed to design BSMs, has led to differences of opinions in the distress mechanisms, especially fatigue versus permanent deformation (Ebels *et al*., 2006), (Twagira *et al*., 2006), (Collings et al. 2011).

The Stellenbosch University has a history of researching the material properties of BSMs in an effort to develop more accurate performance models for bitumen treated materials. Part of this programme is an extensive triaxial test investigation. In the same vein as the methodology followed by Jenkins (2000), this tri-axial investigation to determine the shear properties of the bitumen stabilised materials, has provided reliable performance function and uses three procedures:

- monotonic tests to determine cohesion (C) and friction angle (φ);
- short duration dynamic tests to determine resilient modulus (M_r);
- long duration dynamic tests to determine permanent (plastic) deformation (ε_p).

Ebels and Jenkins (2007) showed the importance of the Deviator Stress Ratio ($\sigma_{d,applied}$ / $\sigma_{d,failure}$) as a key parameter for determining the rate of permanent deformation accumulation . This research verified used long duration tests (up to one million load repetitions or 4% permanent axial strain) to verify a template of permanent deformation rates linked to the Deviator Stress Ratio. Fig. 2 shows the conceptual implementation of this mix design approach in the structural pavement design.

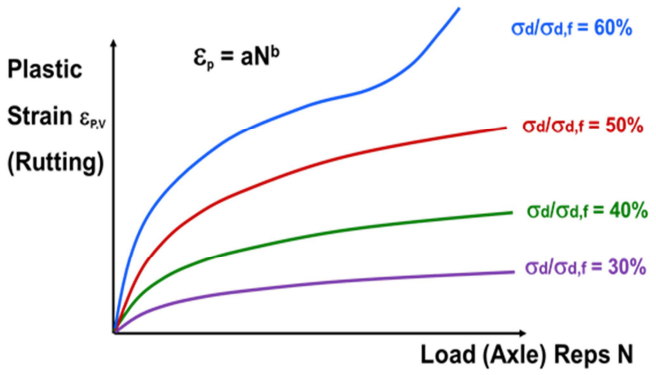

Fig. 2: Permanent deformation for different stress ratios

Mechanistic-empirical analysis provides the major and minor principal stresses in the BSM base layer. These values are analysed together with the shear parameters (Cohesion C and Friction Angle ϕ), to calculate the Deviator Stress Ratio, which in turn determines rate of rutting. Although this approach might appear to be straight forward, this paper explores some of the fundamental, theoretical challenges linked to this technology with more detailed analyses that could lead to more robust analyses.

This paper explores the modelling of a well compacted granular-type and non-continuously bound material with an elastic-plastic model. The purpose of this research was to evaluate the behaviour of an unbound G2 material and compare it with the equivalent foamed bitumen stabilised material (BSM-foam) as defined in TG2 [14]. The same unbound G2 specimen was stabilised as a BSM to simulate practice where the initial base is constructed as a G2 and then after its service life is stabilised to a BSM in a rehabilitation procedure.

II. Material Preparation and Test Protocol

The material modelling in this paper is primarily based on triaxial testing done at the Stellenbosch University. Further guidance will be obtained from results published by Maree (1979) and further augmented by data published by Theyse (2008).

All specimens (300 mm x 150 mm dia.) were conditioned for testing at 50 % of optimum moisture content (OMC = 5.7 %) and compacted to 100 % of Mod. AASHTO dry density (2298 kg/m^3), representing approximately 85 % volumetric density. Specimens were sieved in the required fractions and then reconstituted in accordance with G2 South African specification in order to reduce the number of variables as the material grading can then be assumed to be constant.

Monotonic tests were done under displacement control at a constant displacement rate of 2.4 mm/min to a maximum of 18 mm (6 % strain) or to a limit of a 10 % drop from the maximum load. The latter was done as to measure the unload behaviour as close as possible to the maximum load condition. Five monotonic tests were on the G2 and six on the BSM at confinement pressures of 0 kPa (BSM only), 20 kPa, 50 kPa, 100 kPa, 150 kPa and 200 kPa.

Repeated load testing to determine the resilient modulus was done at five load levels (10 to 50 % of maximum deviator stress in 10% intervals) of 100 cycles each after an initial 1000 cycle conditioning period. The conditioning is done at 100 kPa confinement, where after the repeated load test is started at a confinement pressure of 200 kPa, with 100 cycles at each load level. The procedure is repeated for the reduced confinement pressures at 150 kPa, 100 kPa, 50 kPa and 20 kPa. All repeated load tests are done on one specimen.

Allen [1] showed that the repeated load test can be done on specimen and that the test can be done in any order as far as confinement is concerned. Therefore the procedure described above was adopted on this basis and not verified separately.

Neither the influence of moisture on the material nor the influence of compaction density was investigated as an experimental variable. Both these material properties are key performance variables, but it is assumed that the material will remain within the same operational conditions throughout its life, i.e. the moisture regime is retained in a dry condition

within reasonable limits and the density of the material remains at the same level, with the possibility of minor additional traffic compaction.

The same specimens used for testing G2 material were reworked to prepare BSM specimens.

III. Material Behaviour under Monotonic Loading

Maree [6] published detailed results from monotonic testing done on several granular materials, shown in Fig. 3. The G2 tested and reported in this paper is compared with the results published by Maree [6] to verify the integrity of the results.

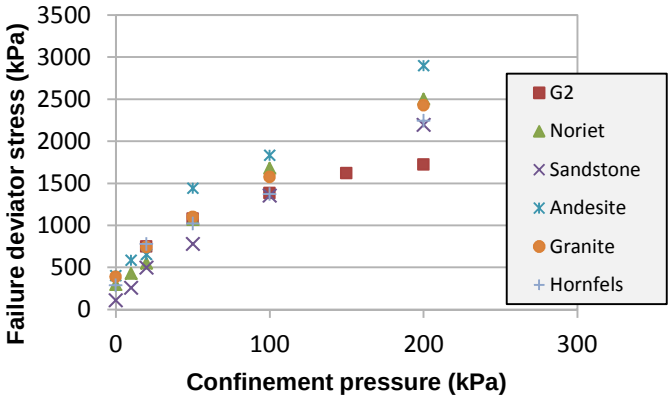

Fig. 3: Monotonic loading results on various materials by Maree [6]

Table 1 shows that the G2 material shear strength compares well with other materials in the low confinement stress ranges, but performs well below the expected strengths at high confinement stress ranges. It is also interesting to note that failure strength of different materials are not highly significant.

Failure strength of the G2 and BSM are compared in Table 1. Both materials were tested up to 200 kPa confinement stresses, but the G2 was not tested at an unconfined state.

Table 1: Comparison of principal stresses at failure for G2 and BSM

Confinement stress σ_3 [kPa]	Principal stress at failure $\sigma_{1,f}$ [kPa]		
	G2	***BSM***	***Ratio***
0	-	1 390.0	-
20	798.1	1 455.5	1.824
50	1 188.8	1 689.0	1.421
100	1 551.1	2 265.4	1.461
150	1 853.6	2 588.6	1.397
200	1 984.1	2 802.1	1.412

Stabilising G2 aggregate with foamed bitumen to produce BSM1 yields the highest benefit in low confinement stress regimes, which is arguably the level of confinement that base courses in most South African pavements are operational.

The monotonic test results for the G2 and BSM at 50 kPa confinement stress are compared in Fig. 4 and Figure 5 on the same vertical and horizontal scales. Estimated linear elastic limits are shown as blue dots, the point of dilation is shown as a red dot and the failure point as a yellow dot.

Comparison of the results shows the significant increase in strength of the stabilised material (BSM) in comparison to the unbound state. However, the BSM is less ductile as the failure (maximum) load occurs at a much lower strain level. Dilation in an unbound material takes place very early in the loading cycle, while it only occurs just before the maximum load is reached in the BSM case. A longer effective compaction regime before dilation takes place for a BSM material is explained with the additional confinement, in terms of internal strength, that is provided by the bounding agent.

The effective linear elastic range for both materials is very small in comparison to the total load capacity. This indicates that plasticity initiates very early in the loading cycle and should be carefully considered.

IV. Plasticity Model

The Mohr-Coulomb model is a very popular and well researched plasticity model used for granular materials. A large database of strength parameters c and φ exists for the Mohr-Coulomb model. In this paper it will be demonstrated that the Desai model can be used to model the failure behaviour of granular materials more realistically.

A. Mohr-Coulomb failure surface

The failure envelope for the Mohr-Coulomb yield surface is given in Eq. (1).

$$f = \tau - c - \sigma_n \tan\varphi \tag{1}$$

From the geometry of the Mohr circle it can be shown that

$$\sin\varphi = \frac{\frac{1}{2}\left(\sigma_{1,f} - \sigma_3\right)}{\frac{c}{\tan\varphi} + \frac{1}{2}\left(\sigma_{1,f} + \sigma_3\right)} \tag{2}$$

resulting in

$$\sigma_{1,f} = \frac{2c\cdot\cos\varphi}{1-\sin\varphi} + \frac{1+\sin\varphi}{1-\sin\varphi}\sigma_3 \tag{3}$$

With σ_{UCS} the unconfined compressive strength and k the triaxial factor, respectively defined as

$$\sigma_{UCS} = \frac{2c\cdot\cos\varphi}{1-\sin\varphi} \tag{4}$$

and

$$k = \frac{1+\sin\varphi}{1-\sin\varphi} \tag{5}$$

Evaluating test data in the $\sigma_1 - \sigma_3$ space allows one to easily calculate σ_{UCS} and k as the failure line is now linear. From these $\sigma_1 - \sigma_3$ values c and φ can easily be calculated as it is no longer necessary to draw circles in a Mohr-diagram and fit a straight line tangent to the circles. It is suggested that more accurate results will be obtained using this method.

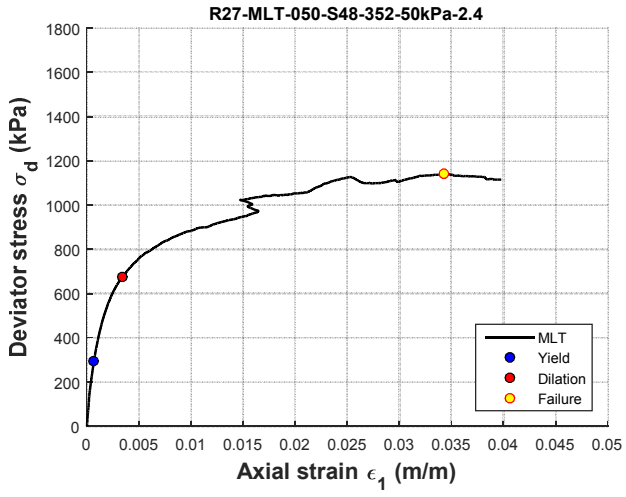

Fig. 4: Monotonic loading on G2 at σ_3 = 50 kPa

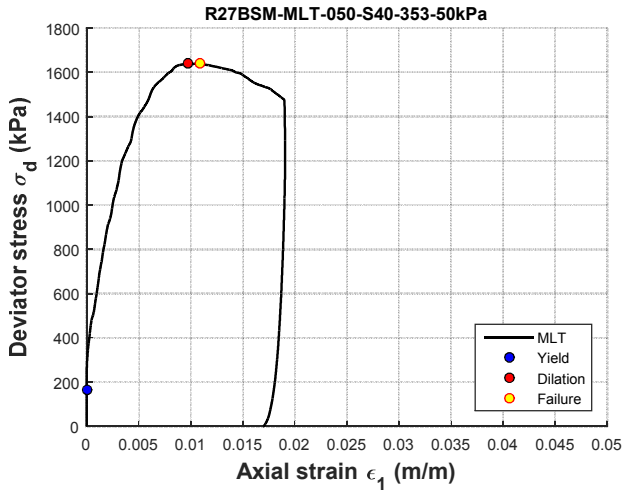

Figure 5: Monotonic loading on BSM at σ_3 = 50 kPa

$$\sin\varphi = \frac{k-1}{k+1} \tag{6}$$

and

$$c = \frac{\sigma_{ucs}\left(1-\sin\varphi\right)}{2\cos\varphi} \tag{7}$$

Test results for the Mohr-Coulomb model in $\sigma_1 - \sigma_3$ space are shown in Fig. 6.

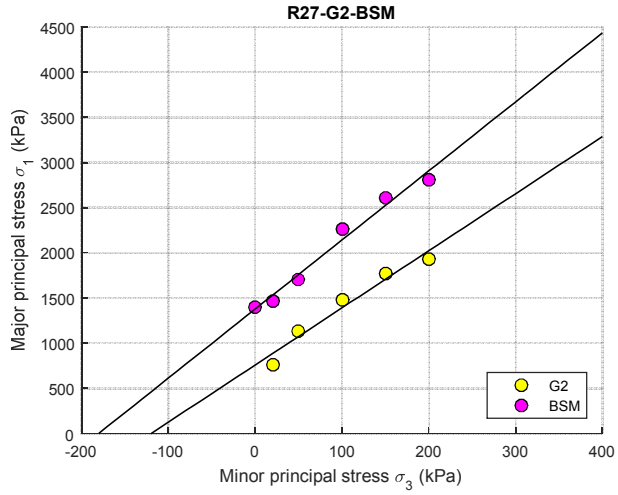

Fig. 6: Mohr-Coulomb model for G2 and BSM

The Mohr-Coulomb parameters determined are summarised in Table 2.

Table 2: Material parameters for Mohr-Coulomb model

Parameter	Mohr-Coulomb model parameters		
	Unit	*G2*	*BSM*
σ_{UCS}	kPa	760.3	1379.4
Triaxial factor, k	-	6.314	7.634
Friction angle, φ	°	46.6	50.2
Cohesion, c	kPa	151.3	249.6

Material parameters Table 2 show that the friction angle of the BSM relative to the G2, has increased by approximately 8% whilst the cohesion has improved by almost 65%. These results are congruent with general findings of BSM material, where the friction often remains relatively constant and sometimes even decreases slightly, but significant increases in shear strength is obtained due to an increase in cohesion.

A high unconfined compressive strength of 760.3 kPa for the neat G2 is reported although it is widely accepted that an unbound granular material does not have an unconfined compressive strength. The 760.3 kPa falls into the C4 class of bound materials. The material was dried back to 50 % of optimum moisture content before testing and the cohesion of 151.3 kPa would be considered as normal. Reporting results as discussed above provides more perspective. Both the cohesion and the unconfined compressive strength must be interpreted as perceived values due to the nature of the linear failure envelope assumed for the Mohr-Coulomb model.

It has been argued by several researchers that a granular material does not have a linear failure envelope and Maree (1979) even proposed a bilinear failure envelope. Inspection of the data shows that the BSM exhibits more of a linear failure envelope than the G2. The G2 tends to reduce in strength at an increased rate at low confinement stresses. Further, the Mohr-Coulomb model has an angular shape in octahedral plane that

makes modelling unstable at these angular edges. A non-linear universal model was proposed by Desai and will be investigated in the next section.

B. Desai failure surface

The failure envelope for Desai, as modified by Liu [5] is shown in Eq. (8).

$$f = \frac{J_2}{p_a} - \left[-\alpha \left(\frac{I_1 + R}{p_a} \right)^n + \gamma \left(\frac{I_1 + R}{p_a} \right)^g \right] \cdot F_s \qquad (8)$$

in which I_1 and J_2 are the first and second stress invariants of the normal and deviator stress tensors respectively, R the triaxial tension and F_s the function related to the shape of the flow surface in the octahedral plane,

$$F_s = \left(1 - \beta \cos 3\theta\right)^m \qquad (9)$$

where

$$\cos 3\theta = \frac{3\sqrt{3}}{2} \frac{J_3}{J_2^{3/2}} \qquad (10)$$

in which J_3 is the third invariant of the deviator stress and θ is equivalent to the Lode angle. The m in Eq. (9) is found to be equal to -0.5 for many geological materials (Liu et al [5]).

The parameter β determines the shape of the failure surface in the octahedral plane and a value of $\beta = 0$ will result in a circular surface in the octahedral plane. For the sake of simplicity in this paper it will be assumed that $\beta = 0$.

Eq. (8)can be expressed in the $p-q$ space for triaxial conditions as is shown in Eq. (11).

$$f = \frac{q^2}{3p_a^2} - \left[-\alpha \left(\frac{3p'}{p_a} \right)^n + \gamma \left(\frac{3p'}{p_a} \right)^g \right] \qquad (11)$$

A detailed discussion of the Desai model is given by Liu [5].

With $\alpha = 0$ in Eq. (11) the maximum failure surface is achieved. Therefore the best fit through the data then only needs to be done with:

$$f = \frac{q^2}{3p_a^2} - \gamma \left(\frac{3p'}{p_a} \right)^g = 0 \qquad (12)$$

From Eq. (12) γ and g is the determined through a log-log linear fit.

The full Desai model parameters are shown in Table 3.

Table 3: Material parameters using Desai model

Parameter	Desai model parameters		
	Unit	*G2*	*BSM*
R	kPa	151.3	290.000
α	-	Varies	Varies
γ	-	0.351	0.420
g	-	1.775	1.776
n	-	2.000	2.000

The Desai model is demonstrated in Fig. 7 using the principal stress space $\sigma_1 - \sigma_3$.

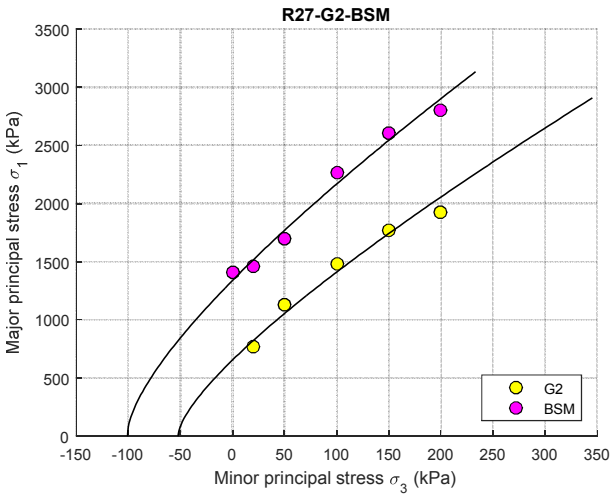

Fig. 7: Desai model for G2 and BSM shown in principal stress space

Note: σ_1 in the graph should be interpreted as $\sigma_{1,f}$, the principal stress at failure.

Fig. 7 shows that the nonlinear failure envelope is now modelled more realistically. Realistic confinement stresses at zero load of approximately 50 kPa for the G2 and 100 kPa for the BSM is predicted, these stresses can be seen as the material's tensile strength capacity, caused by suction in the case of the G2 and suction and bounding in the case of the BSM.

It is customary to operate the Desai model (or for that matter any plasticity model) in the $I_1 - \sqrt{J_2}$ space. However, engineers are more familiar with the $p-q$ space, with $p = \left(\sigma_1 + 2\sigma_3\right)/3$ and $q = \sigma_1 - \sigma_3$. Fig. 8 shows the Desai model in the $p-q$ space.

Modelling the hardening and softening behaviour of a material with a Mohr-Coulomb model can only be achieved by manipulating either c or φ, or both. The most popular method is to manipulate c which is similar to manipulating α in the Desai model, except that the nonlinear behaviour shown in Fig. 9 is lost as only a linear relationship can be represented by a Mohr-Coulomb model.

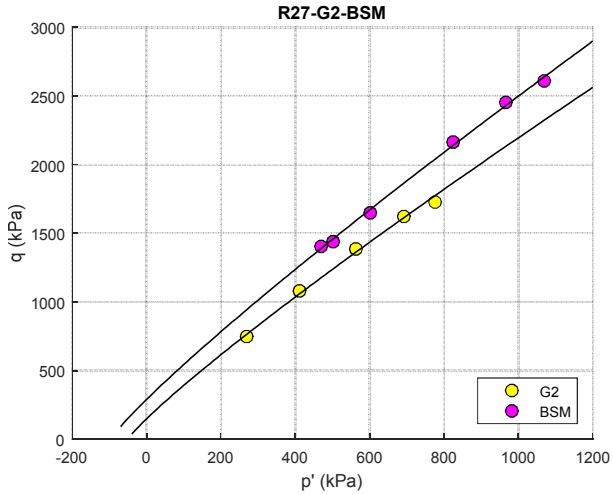

Fig. 8: Desai model for G2 and BSM shown in p-q space

The Desai parameter α, is used to model the hardening and softening behaviour of a material, as illustrated in Fig. 9.

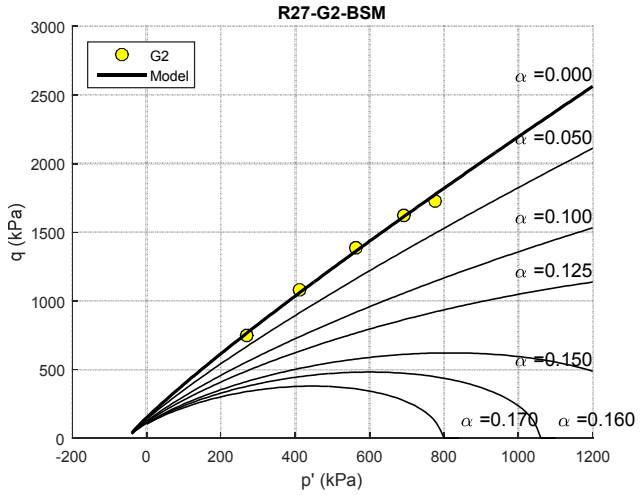

Fig. 9: Hardening (softening) model for G2 using Desai

It has been shown that a nonlinear approximation of the failure envelope for a granular material yields a more realistic model. The Desai model is sufficiently simplistic to be implemented in finite element routines. Hardening and softening can be modelled adequately and the shape of the failure envelope in the deviatory plane is smooth that is a great benefit over the Mohr-Coulomb model.

V. Material Behaviour under Repeated Loading

Granular materials undergo plastic deformation during each load application; however, after a certain number of load applications at a certain load level the deformation stabilise to a constant rate. At this point the granular material is an almost elastic an exhibits elastic behaviour, described as the resilient state. Resilience is the property of a material that allows absorption of energy when it is deformed elastically. Then, upon unloading, this energy is recovered. The elastic modulus taken at this point is defined as the resilient modulus as is illustrated in Fig. 10.

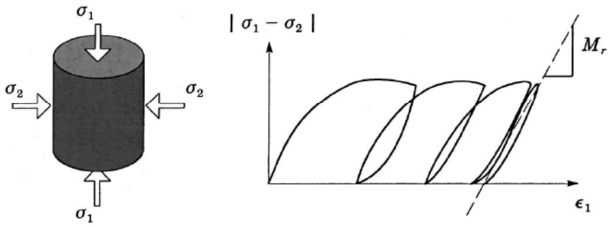

Fig. 10: Typical resilient behaviour yielding a resilient modulus ([8])

The granular material behaviour during one load cycle is demonstrated in Fig. 11. There is a difference in the loading path and the unloading path, with the difference implying a dissipation of energy during the load cycle. At the end of the load cycle a certain amount of resilient strain is recovered and the total strain minus the resilient strain is the permanent deformation experienced during the load cycle.

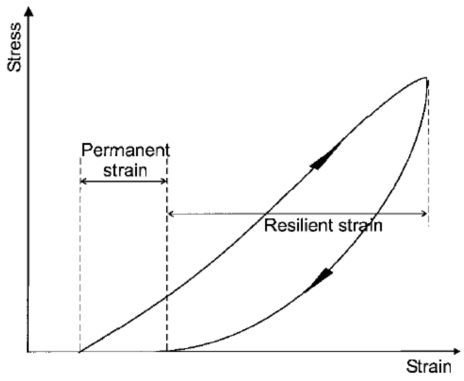

Fig. 11: Stress/strain behaviour during one loading cycle

The resilient modulus is defined as

$$M_R = \frac{\sigma_d}{\varepsilon_r} \tag{13}$$

with σ_d the deviator stress and ε_r the recoverable (resilient) axial strain.

The resilient behaviour of the G2 and BSM materials are demonstrated in Fig. 12 and Fig. 13 respectively, where the last five loading cycles are compared with the first five loading cycles during 500 load cycles of the permanent deformation conditioning test. Almost no permanent deformation is observed during the last five cycles of both the G2 and BSM, yet permanent deformation of 0.74% and 0.35% occurred during the 500 load applications for the G2 and BSM respectively. The BSM displays a significantly higher resistance to permanent deformation due to the stabilising done to obtain a bound material.

Resilient modulus is often modelled with the Uzan-model ([10], [11][12]) as defined in Eq. (14).

$$M_R = k_1 \left(\frac{I_1}{p_a} \right)^{k_2} \left(\frac{J_2}{p_a^2} \right)^{k_3} \quad (14)$$

with k_n model parameters and p_a the atmospheric pressure, taken as 101.325 kPa (at sea level). It should be noted that any reference pressure can actually be taken, such as 1 kPa, with the only difference that the model parameters will differ. The Uzan model was fitted to the data and is shown in Table 4 and Table 5.

Table 4: Uzan model for G2 material

Confinement (kPa)	Uzan model parameters			
	k_1	k_1	k_1	r^2
20	89.023	1.7264	-0.4623	0.999
50	54.338	1.6308	-0.2667	1.000
100	15.154	2.0910	-0.2884	0.991
150	7.250	2.2983	-0.3351	0.966
200	22.944	1.6797	-0.2876	0.987
All	255.394	0.4256	-0.0577	0.673

Table 5: Uzan model for BSM material

Confinement (kPa)	Uzan model parameters			
	k_1	k_1	k_1	r^2
20	2.425	6.0631	-2.6027	0.998
50	9.444	3.0473	-0.9868	1.000
100	5.621	2.7899	-0.7367	0.995
150	6.524	2.4954	-0.6224	0.976
200	33.546	1.6689	-0.4616	0.989
All	138.179	0.8197	-0.2208	0.700

The individual models fitted to the different confinement stress levels gave very good results. However, if the Uzan model is fitted to the total dataset the fit is not good.

It should be noted that more sophisticated models were developed during South African Pavement Design Method (SAPDM) research and will be reported elsewhere. Further details will also be available during the SARDM Workshop following CAPSA 2015. Insufficient variables were tested during this research to be able to fit the SAPDM models.

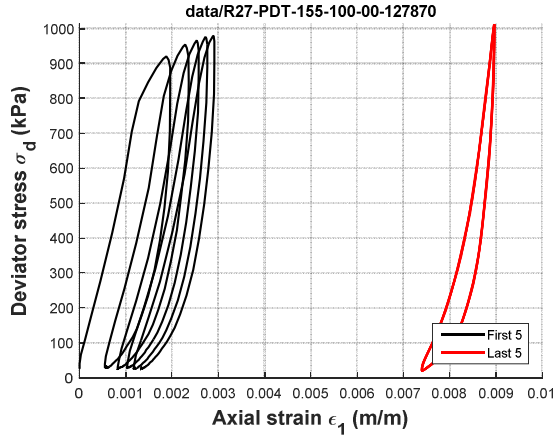

Fig. 12: Resilient behaviour of G2 (conditioning stage)

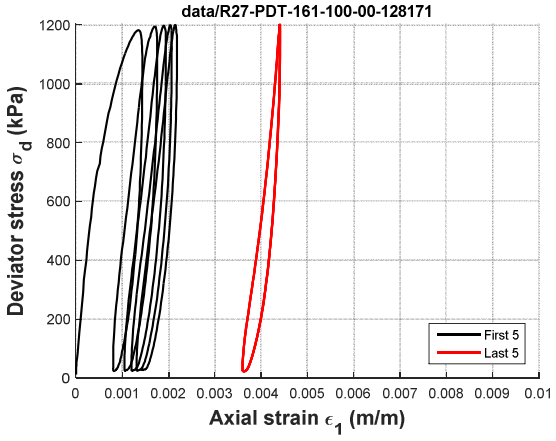

Fig. 13: Resilient behaviour of BSM (conditioning stage)

VI. PERMAMNENT DEFORMATION

The deformation behaviour of a granular material under cyclic loading was already referred to above. The permanent deformation during a load cycle can be considered to be a consequence of compaction, consolidation and a distortion process of the internal fabric and possibly the deformation and/or disintegration of the individual grains.

The permanent deformation of the G2 and BSM are compared in Fig. 14 and Fig. 15 and the volumetric behaviour in Fig. 16 and Fig. 17. Much less permanent deformation is experienced with the bound BSM compared to the unbound G2. What is interesting is that G2 dilates while the BSM does not show any indication of dilation. Only one specimen at a confinement stress of 100 kPa was tested due to the limited availability of the triaxial equipment.

After conditioning the actual permanent deformation test commences. During the first 10 min every load cycle is recorded, for the next 50 minutes the last five cycles of every 5 minutes are recorded, the next 60 minutes the last five cycles of every 10 minutes and the last five cycles of every 20 minutes is recorded for the rest of the test.

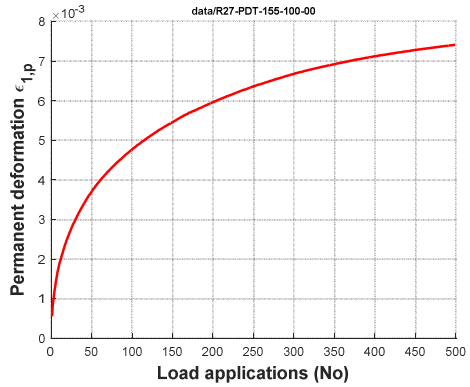

Fig. 14: Permanent deformation during conditioning of G2

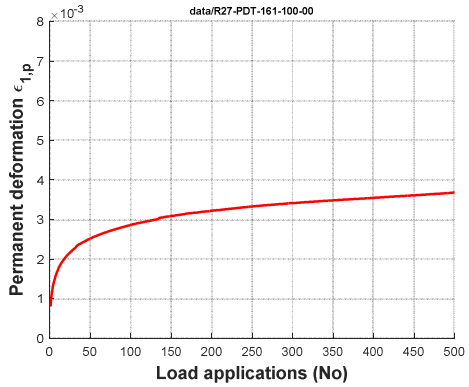

Fig. 15: Permanent deformation during conditioning of a BSM

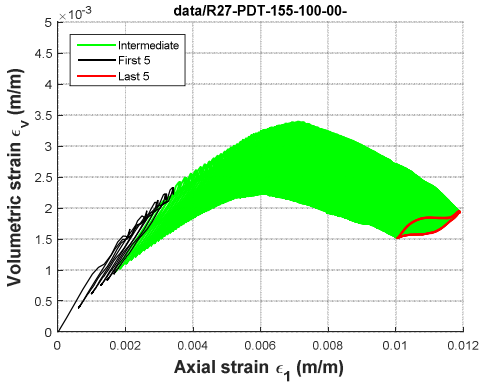

Fig. 16: Volumetric behaviour during conditioning of G2

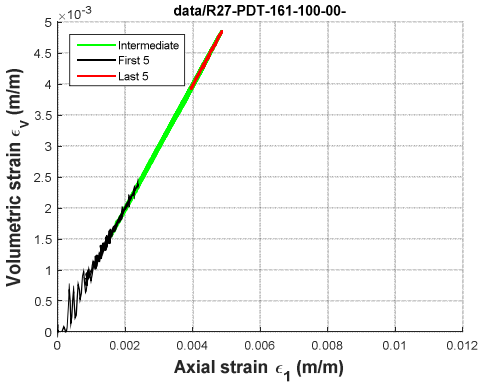

Fig. 17: Volumetric behaviour during conditioning of BSM

The permanent deformation of the G2 and BSM during normal permanent deformation test procedure, later referred to as Stage 1 loading, are compared in Fig. 18 and Fig. 19 and the volumetric behaviour in Fig. 20 and Fig. 21. Much less permanent deformation is again experienced with the bound BSM compared to the unbound G2. Now negative dilation is experienced with the G2 and the same trend is followed from hereon as the BSM. Volumetric changes in the BSM are significantly less than the G2 and are consistently linear in nature. During Stage 1 loading the deformation rate becomes constant towards the latter part of the loading cycles. 76 800 and 72 000 load cycles were applied to the G2 and BSM respectively, which is substantially more than the 50 000 normally applied. Standard practise is to determine the constant deformation rate after 50 000 load cycles and extrapolate the deformation to a standard (10 mm for Class 1 roads) to determine the bearing capacity of the material.

The characteristic behaviour of a granular material is that an accelerated deformation rate is experienced during the early stages of loading. This is again clearly demonstrated in Fig. 18 and Fig. 19 where the majority of the deformation takes place in the first 1000 load applications. Thereafter the deformation rate reduces to a constant rate from which the material's life can be predicted, as compared to a standard max terminal deformation. Assuming a terminal condition of 10% strain, i.e. 15 mm deformation on a 150 mm thick layer, translates into pavement lives of 18.6 and 24.1 million load applications for a G2 and BSM respectively. The original pavement life is therefore extended with at least the same life expectancy as the original pavement, without any intrusive construction actions, only a standard in-situ recycling operation is required with minimal inconvenience due to traffic accommodation. This assumption also excludes moisture resistance considerations and durability benefits of the BSM.

It should be noted that the G2 was tested at a stress ratio, $\sigma_d / \sigma_{d,f}$ = 0.66 while the BSM was tested at lower stress ratio of 0.54 during this Stage 1 loading, see Table 6.

In an effort to introduce catastrophic failure to establish the ultimate bearing capacity of the road it was decided to introduce a stage loading concept where the stress ratio is progressively increased until catastrophic failure is reached. This was done for the two materials as is depicted in Table 6. It can be seen that the G2 material was subjected to an initial stress ratio of 0.66 of the monotonic failure load (1 551.1 kPa from Table 1) up to a maximum of 0.94 at which stage the deformation rate accelerated considerably. Similarly the BSM was initially subjected to a stress ratio of 0.54 of the monotonic failure load (2 265.4 kPa from Table 1). After each load increase the initial accelerated deformation rate is observed followed by the characteristic plateau of constant deformation rate.

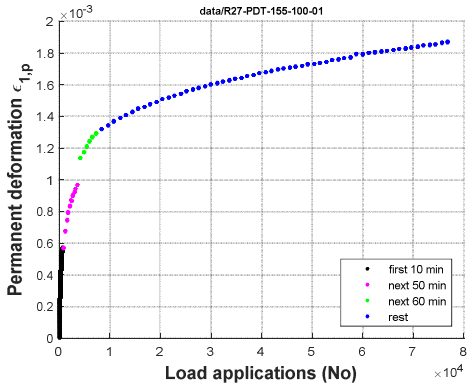

Fig. 18: Permanent deformation during Stage 1 loading G2

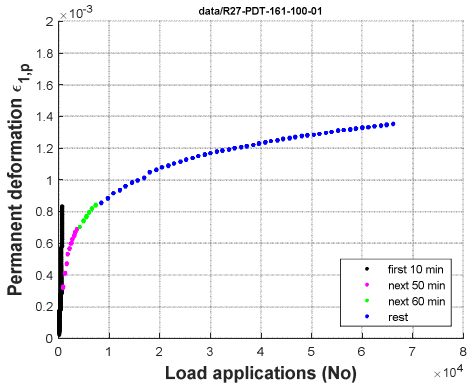

Fig. 19: Permanent deformation during Stage 1 loading BSM

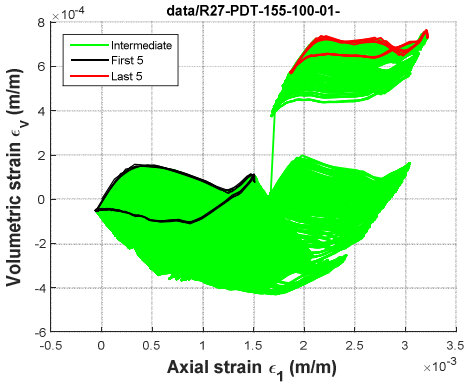

Fig. 20: Volumetric behaviour during Stage 1 loading G2

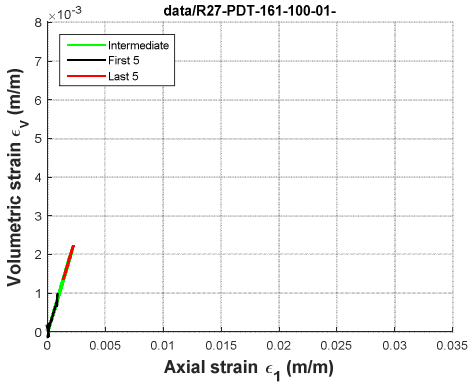

Fig. 21: Volumetric behaviour during Stage 1 loading BSM

Table 6: Stage loading and load levels per stage

Stage	G2			BSM		
	Loads	σ_d	Stress ratio	Loads	σ_d	Stress ratio
1	76 800	1 018.1	0.66	72 000	1 201.8	0.54
2	74 405	1 122.4	0.72	76 805	1 299.5	0.57
3	64 805	1 235.0	0.80	68 405	1 412.4	0.62
4	49 205	1 348.0	0.87	64 805	1 525.3	0.67
5	52 805	1 459.6	0.94	81 605	1 638.1	0.72

The constant deformation rates at the different load levels are shown in Table 7

Table 7: Deformation rate at different load levels

Stage	G2		BSM	
	Stress ratio	Deterioration rate (x 10^{-6})	Stress ratio	Deterioration rate (x 10^{-6})
1	0.66	0.005273	0.54	0.004087
2	0.72	0.003625	0.57	0.003084
3	0.80	0.004052	0.62	0.003656
4	0.87	0.008696	0.67	0.007333
5	0.94	0.029400	0.72	0.009193

As only one specimen was tested it was necessary to really approach this method with care. This is not a standard test and with no experience one can easily overload the specimen too early. The G2 was tested first and it was decided that the BSM would be started at a lower initial stress ratio as a BSM is more sensitive to high stress ratios than a neat G2.

The deformation rates of the G2 and BSM are compared in Fig. 22 where it is clear that the deformation rate of a G2 starts to rapidly increase at stress ratios above 0.8, with a BSM more sensitive with an increase in deformation rate from stress ratios above 0.65. This is consistent with more conventional permanent test done.

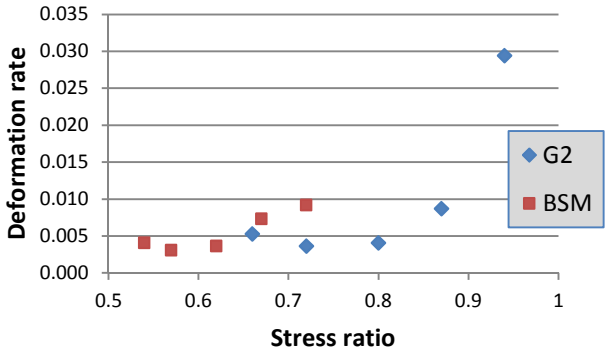

Fig. 22: Deformation rate at different load levels

The complete stage loading permanent deformation test of the G2 and the BSM is compared in Fig. 23 and Fig. 24.

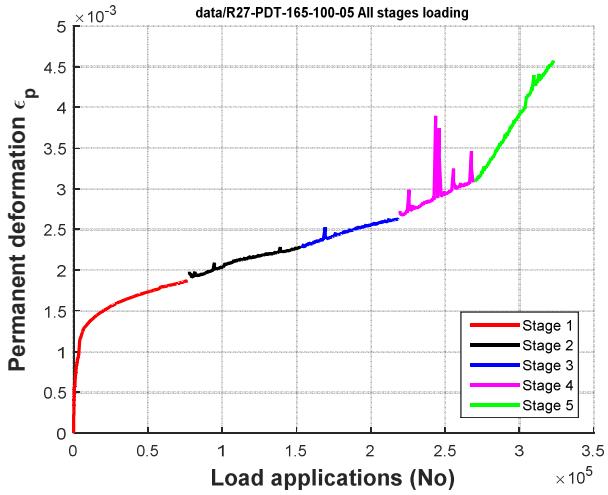

Fig. 23: Stage loading PD test of a G2

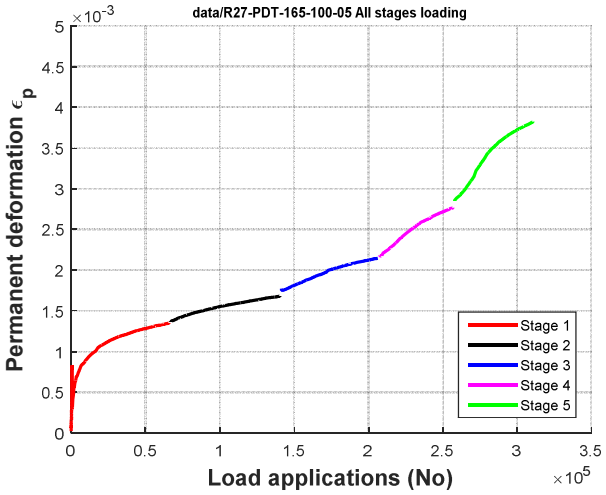

Fig. 24: Stage loading PD test of a BSM

VII. Conclusions and Implications

Monotonic Loading

- The Desai model in the principal stress space provides a more realistic non-linear failure envelope for granular materials. This is relevant to high quality granular base materials, but is less relevant to BSM, which is has a more linear failure envelope.

Dynamic Loading (Resilience)

- Both granular materials and BSM show significant reduction in plastic behaviour within the first 500 loading cycles, at a constant loading level. The BSM, however, provides significantly higher resistance to plastic deformation.

Dynamic Loading (Permanent Deformation)

- Staged loading at increasing stress levels shows a 30% extension of the life of a base through bitumen stabilisation, in terms of resistance to permanent deformation, based on the analysis one a G2 material and an equivalent BSM. This excludes additional benefits of bitumen stabilisation i.e. moisture resistance and durability.

Acknowledgements

This paper is presented with the approval of the South African National Roads Agency SOC Limited. The contents of the paper reflect the views of the authors who are responsible for the facts and accuracy of the data presented herein. The contents do not necessarily reflect the official view or policies of the South African National Roads Agency SOC Limited. Haw & Inglis is thanked for provision of materials. Aisha Solomon and Achille Nwando are thanked for extensive laboratory work.

References

[1] Allen, J.J. "The effects of non-constant lateral pressures on the resilient response of granular materials". PhD Dissertation. University of Illinois, Urbana, Illinois. United States of America. 1973.

[2] Committee of State Road Authorities (CSRA), TRH 14: 1985. "Guidelines for Road Construction Materials". Department of Transport, South Africa. 1985.

[3] Committee of State Road Authorities (CSRA), TRH 4: 1996. "Structural Design of Flexible Pavements for Interurban and Rural Roads". Department of Transport, South Africa. 1996.

[4] Heath, A.C. "Modelling unsaturated granular pavement materials using bounding surface plasticity". PhD Dissertation. University of California, Berkeley. United States of America. 2002.

[5] Liu, X., Cheng, X.H., Scarpas, A. and Blaauwendraad, J. "Numerical modelling of nonlinear response of soil. Part 1: Constitutive model". International Journal of Solids and Structures. Volume 42, p1849-1881. 2005.

[6] Maree, J.H. "Die resultate van eenmalige belasting en herhaalde belasting drie-assige skuiftoetse op 'n reeks klipslag en gebreekte klip kroonlaagmateriale". Tegniese verslag RP/12/78. WNNR, Suid-Afrika. 1979.

[7] Scarpas, A. "A Mechanics based Computational Platform for Pavement Engineering". PhD Dissertation. Delft University of Technology. The Netherlands. 2004.

[8] Taciroglu, E. "Constitutive Modelling of the Resilient Response of Granular Solids". PhD Dissertation. University of Illinois, Urbana, Illinois. United States of America. 1998.

[9] Theyse, H.L. "A Mechanistic-empirical Design Model for Unbound Granular Materials". D.Eng Dissertation. University of Johannesburg. South Africa. 1994.

[10] Uzan, JL. "Characterization of Granular Material". Transportation Research Record 1022, Transportation Research Board, Washington, D.C., p52-58. 1985.

[11] Uzan, JL. "Resilient Characterization of Pavement Materials". International Journal for Numerical and Analytical Methods in Geomechanics, Vol 16, p543-459. 1992.

[12] Uzan, JL. "Permanent Deformation in Flexible Pavements". Journal for Transportation Engineering, Vol 16, p543-459,ASCE. 2004

[13] Wolff, H. "Elast-Plasto modelling of granular layers". Research Report RR92/913, Department of Transport, South Africa. 1992.

[14] Jenkins KJ, Collings DC, and Long FM (main authors) with contributions from Jooste F, Grobler J, Hughes M, J and Thomson H. *Technical Guideline TG2: Bitumen Stabilised Materials: A Guideline for the Design and Construction of Bitumen Emulsion and Foamed Bitumen Stabilised Materials.* Second Edition. Published by Asphalt Academy. May 2009. ISBN 978-0-7988-5582-2. Pages 136

[15] M. Young, The Technical Writer's Handbook. Mill Valley, CA: University Science, 1989.